

# Marine Accident Integrated Analysis System using Highly Advanced M&S System of FSI Analysis Technique

Sang-Gab Lee, Jae-Seok Lee, Ji-Hoon Park and Tae-Young Jung

Korea Maritime & Ocean University, Marine Safety Technology, Busan, Korea

## 1 Abstract

Investigation of marine accident causes usually depends on the judgments of maritime experts, based on the statements of the concerned persons in the case where there is no navigation equipment, such as AIS and VDR. Scientific verification also has a limitation in the case of their conflicting statements. It is necessary to develop Marine Accident Integrated Analysis System (MAIAS) using highly advanced Modeling & Simulation (M&S) system of Fluid-Structure Interaction (FSI) analysis technique for the scientific investigation of marine accident causes and for the systematic reproduction of accident damage procedure. To ensure an accurate and reasonable prediction of marine accident causes, full-scale ship collision, contact, grounding, flooding, capsizing, sinking and turning simulations would be the best approach using hydrocode, such as LS-DYNA, with its FSI analysis technique, propulsion force for ship velocity, and rough sea weather such as current, strong wind and wave with irregular spectrums. The objective of this paper is to present the findings from full-scale ship collision, grounding, flooding, capsizing, sinking and rapid turning simulations of marine accidents, and to demonstrate the feasibility of the scientific investigation of marine accident causes using MAIAS.

**Keyword Words:** *Marine Accident Intergated Analysis System (MAIAS), Highly Advanced Modeling & Simulation (M&S) System; Fluid-Structure Interaction (FSI) Analysis Technique; Full-Scale Ship Collision, Contact, Grounding, Flooding, Capsize, Sinking and Rapid Turning Simulations; LS-DYNA code.*

## 2 Introduction

It has been reported, from the statistics of marine accidents by the Korean Maritime Safety Tribunal (KMST) and the Lloyd's Maritime Information Services (LMIS), that collision, grounding, contact, capsizing and sinking accidents compose a majority of marine accidents, as shown in Fig. 1, bringing about a great loss of life and property, and ocean environment due to oil spills. Investigation of marine accident causes usually depends on the judgments of maritime experts, based on their shipping experiences and the statements of the concerned persons in the case of no navigation equipment, such as AIS and VDR. Scientific verification also has a limitation in the case of their conflicting statements. It is necessary to develop highly advanced Modeling & Simulation (M&S) system using Fluid-Structure Interaction (FSI) analysis technique for the scientific investigation of marine accident causes and for the systematic reproduction of accidents damage procedure.

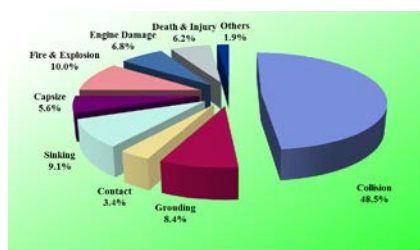


Fig. 1: Marine accidents according to type [1]

With the advent and ongoing advances in numerical simulation capabilities and its sophisticated tools, such as highly accurate dynamic nonlinear simulation hydrocode LS-DYNA [2], development of crashworthiness analysis techniques has been actively carried out using highly advanced M&S system for car design and accident cause investigation with viable, less costly alternatives as well as more reliable aids to the tests and/or experiments. Several interaction effects in the seawater should be

considered contrary to the car collision and plane crash accidents due to high density (1,000 times) of seawater compared to that of air (1 time), such as floating, motion, inboard flooding, wave making, squeezing pressure, and bank effect, etc. To ensure an accurate and reasonable investigation of marine accident cause, such as collision, contact, grounding, flooding, capsizing, sinking and rapid turning, etc., full-scale simulations would be the best approach using highly advanced M&S system with FSI analysis technique of hydrocode LS-DYNA. This system could be denominated as Marine Accident Integrated Analysis System (MAIAS) including propulsion force for the real ship velocity, and rough sea weather, such as current, strong wind and wave with irregular spectrums, since the cause investigation of most marine accident types could be handled except engine damage one. Fracture criteria has to be also suitably applied to the structural damage considering strain rate effect, together with careful investigation of damage information.

FSI problems could be conveniently simulated by the moving mesh algorithm and overlap capability of grid to structure mesh using Multi-Material Arbitrary Lagrangian Eulerian (MMALE) formulation and Euler–Lagrange coupling algorithm of LS-DYNA code, as shown in Fig. 2. This coupling algorithm would be more suitable for the FSI problems with very complicated deformable structure. Volume Of Fluid (VOF) method is adopted for solving a broad range of nonlinear free surface problems [3, 4]. The objective of this paper is to present several cases of full-scale ship collision, grounding, flooding, capsizing, sinking and rapid turning simulations of marine accidents, and to demonstrate the feasibility of the scientific investigation of marine accident causes using MAIAS.

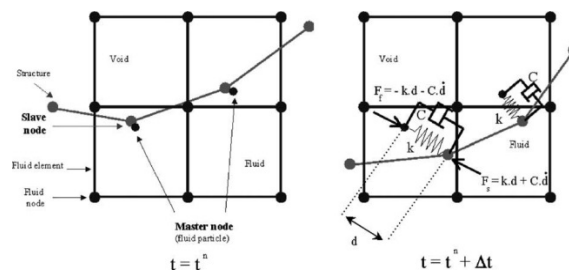


Fig.2: Sketch of penalty coupling algorithm [3]

### 3 Internal Damage Mechanics

1:5 scale grounding test results of NSWC [5] are usually used for the verification of F.E. simulation capability and fracture criteria, as shown in Fig. 3. One of grounding test models, ADH/PD328V, was simulated using rough and fine mesh models with failure strains from 0.20 to 0.35, as shown in Fig. 4, and material properties of ASTM 569, as shown in Table 1. It was found that failure strain 0.3 and 0.2 were suitable for the fine and rough meshes with ratio 12.5 and 25.0 of finite element size to thickness, respectively. Failure strain would be determined by ratio of finite element mesh size to its thickness in the crashworthiness analysis [6].

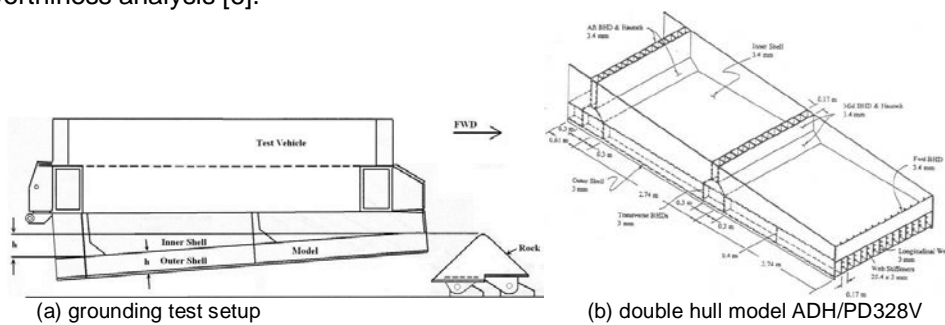
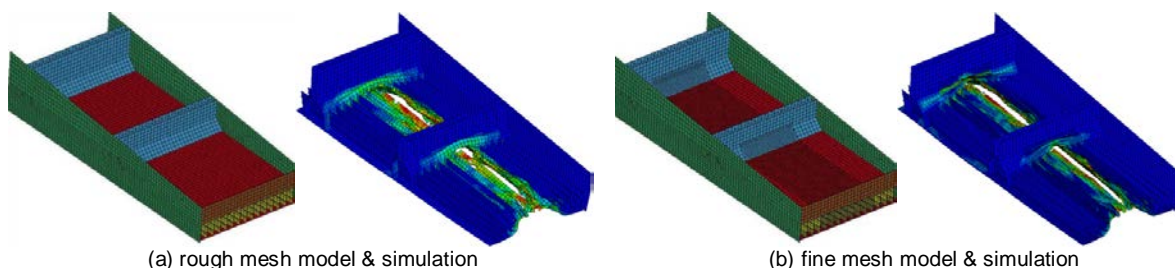


Fig.3: Grounding test setup and model of NSWC [5]



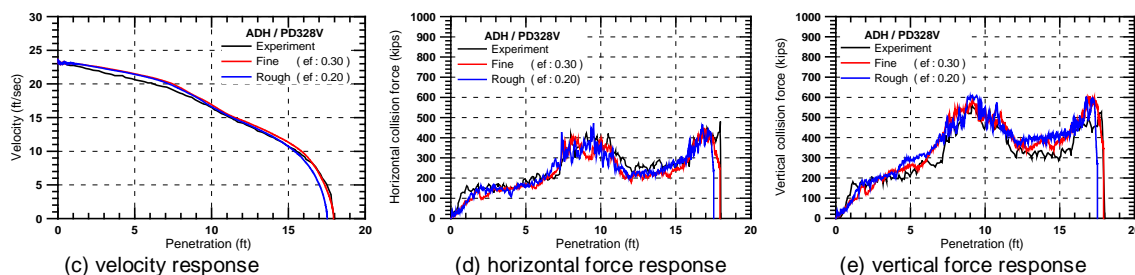


Fig.4: Grounding test simulation of ADH/PD328V model

Table 1: Material properties of ASTM 569

Property	ASTM 569
Young's modulus (ksi)	$3.00 \times 10^7$
Density (lbf-s <sup>2</sup> /in)	$7.43 \times 10^{-4}$
Poisson's ratio	0.30
Yield & Ultimate stresses (ksi)	41.00 & 50.00
Failure strain	0.20, 0.25, 0.30, 0.35
Dynamic yield stress constants	$D=40.4 \text{ s}^{-1}$ , $q = 5$

## 4 Full-Scale Ship Simulations using MAIAS

Full-scale ship collision, grounding, flooding, sinking and rapid turning simulations were carried for the cause investigation of marine accidents, and some of their cases are represented for the demonstration of the feasibility of the scientific investigation of marine accidents and reasonable structural safety assessment using MAIAS.

### 4.1 Investigation of collision accident of small fishing ship

Fishing vessel with G/T 124 ton was struck and sunk down to the bottom of river by the large cargo ships with G/T 4,000 ton and over. The collision accident occurred during cross of the struck ship to the path of the striking ships. Figure 5 shows the collision scenario and modeling of full-scale ship collision & sinking simulation, and damage configuration of struck fishing vessel. In this study, among several scenarios, one collision simulation one was considered, such as collision attack angle 80°, striking and struck ship velocities 7 and 5 knots, respectively, as shown in Fig. 5(b). For the comparison of simulation results using FSI analysis technique with those of conventional one, full-scale collision simulation was carried in void condition with the consideration of added mass, such as 1.1 times for the striking ship and 1.8 times for the struck one, where collision velocities were initial ones. Material properties of mild and high tensile steels for the striking and struck ships are summarized in Table 2.

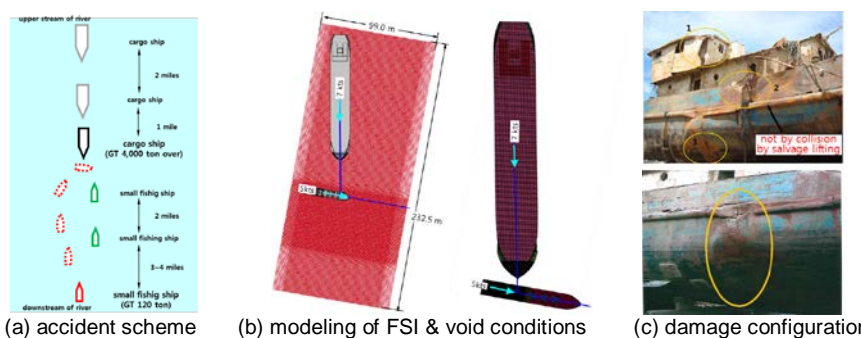


Fig.5: Scenario and modeling of full-scale ship collision &amp; sinking simulation, and damage configuration

Table 2: Material properties of mild and high tensile steels

Property	Mild Steel	High Tensile Steel
Young's modulus (GPa)	206.0	206.0
Density (kg/m <sup>3</sup> )	7,850	7,850
Yield & Ultimate stresses (MPa)	235.0 & 445.0	315.0 & 525.0
Failure strain	0.20, 0.25, 0.30	0.20, 0.25, 0.30
Dynamic yield stress constants	$D=40.4 \text{ s}^{-1}$ , $q=5$	$D=24,804.6 \text{ s}^{-1}$ , $q=5$

Figures 6 and 7 show the full-scale ship collision, capsize & sinking simulation behaviors and collision damage responses (stress responses) of struck fishing vessel using FSI analysis technique against the cargo ships with vertical and bulbous bows, respectively. It could be found that collision damage of struck fishing vessel looks like almost the same regardless of bow types of striking cargo ships, and that their simulation damage is also similar to the real damage one, as shown in Fig. 5(c). This is due to the fact that fishing vessel was too small to be collided to the top portion of vertical or bulbous bows of cargo ships, right after collision to the inclined bow flare, since fishing vessel was floating. Its side main deck and low side shell plate was continuously collided to the bow flare part of cargo ships, and was escaped from the their bow flare and capsized, as realistic behavior.

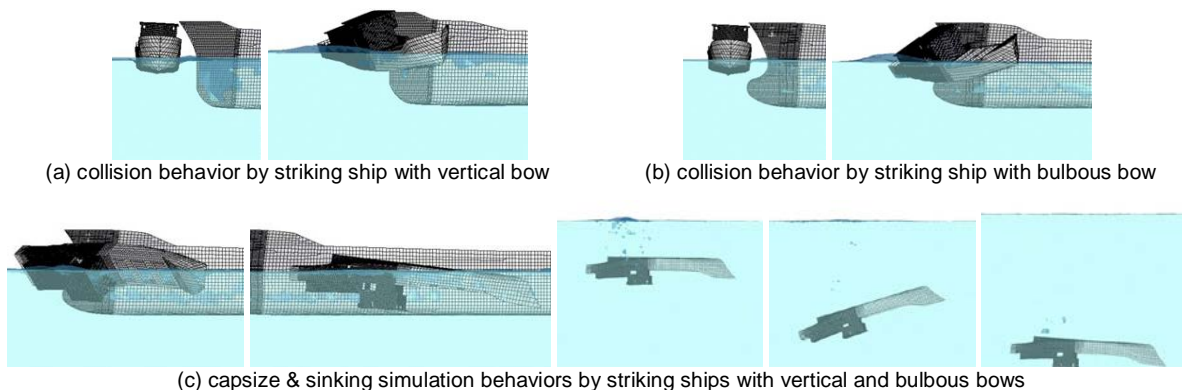


Fig.6: Full-scale ship collision, capsize & sinking simulation behaviors using FSI analysis technique

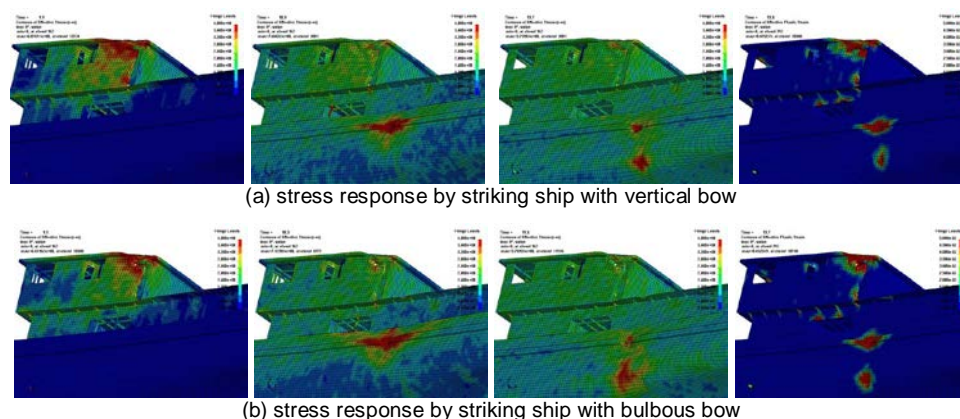
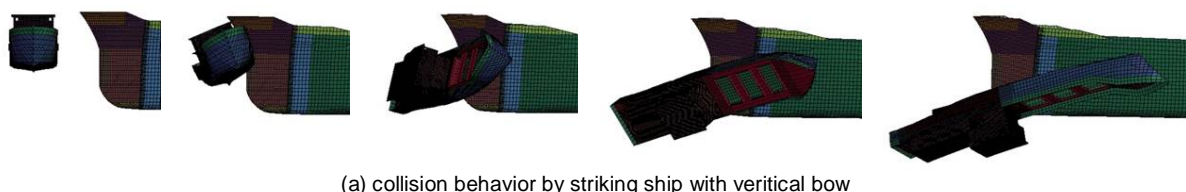


Fig.7: Collision damage responses in full-scale ship collision simulation using FSI analysis analysis

Figures 8 and 9 illustrate the full-scale ship collision & capsize simulation behaviors and collision damage responses (stress responses) of struck fishing vessel using void condition with initial velocity against the cargo ships with vertical and bulbous bows, respectively. It could be found that collision damages of struck fishing vessel look like unrealistic and different depending on the bow types of striking cargo ships, and that their simulation damages are not similar to the real damage one, as shown in Fig. 5(c). Fishing vessel was rebounded downward right after collision to the inclined bow flare, since there was no buoyance in the void condition. While the bottom of fishing vessel was collided to the top of bulbous bow of cargo ship and then rebounded upward, the low side shell plate of fishing vessel was collided along to the vertical bow of cargo ship. All damage of fishing vessel was followed by its collision behavior according to the bow type of cargo ships. It could be found that more accurate and realistic collision behaviors could be realized using FSI analysis technique.



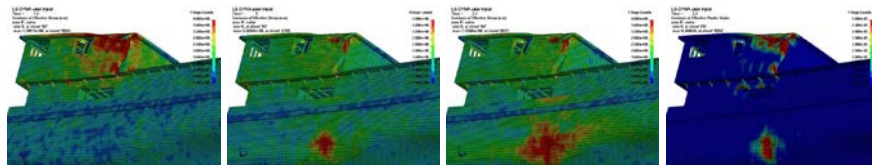
(a) collision behavior by striking ship with vertical bow



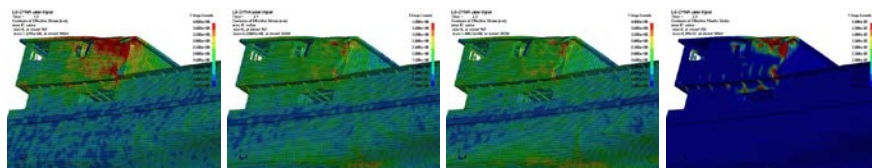


(b) collision behavior by striking ship with bulbous bow

Fig.8: Full-scale ship collision & capsizing simulation behaviors in void condition



(a) stress response by striking ship with vertical bow

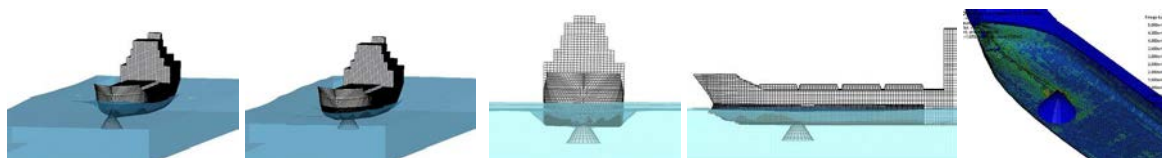


(b) stress response by striking ship with bulbous bow

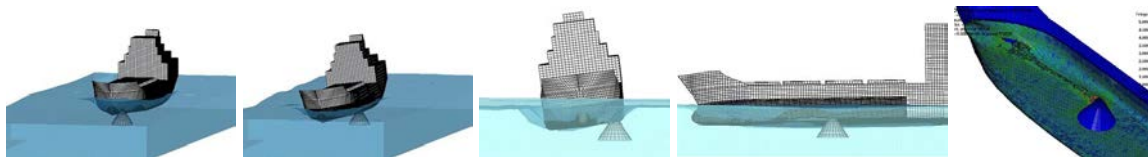
Fig.9: Collision damage responses in full-scale ship collision simulation in void condition

#### 4.2 Grounding safety assessment of specialized ship

Full-scale grounding simulation of the specialize ship with DWT 2,600 ton was performed for its structural safety assessment using FSI analysis technique and applying propulsion force to ship. Two grounding scenarios were considered according to rock position, center of the longitudinal line and 3.0m off the longitudinal one, with full loading condition. In this study mild and high tensile steels were used for the specialized ship, as shown in Table 2. Figure 10 illustrates the full-scale ship grounding simulation behaviors, with two rock positions, center of and 3.0 m off the longitudinal center line, using FSI analysis technique. Realistic grounding simulation behaviors and bottom damage configurations of the ship, such as jumping and sway around the rock under the self-weight of grounding ship, could be found depending on the rock position.



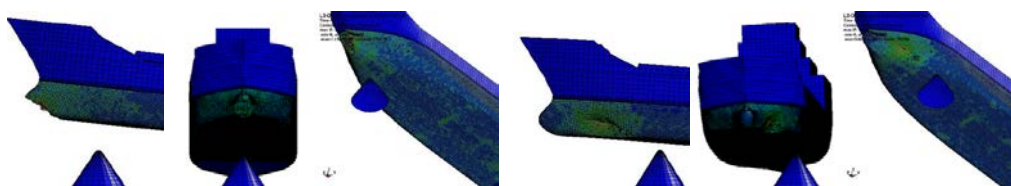
(a) grounding behavior at rock position center



(b) grounding behavior at rock position 3.0 m off

Fig.10: Grounding simulation behaviors according to rock position using FSI analysis technique

Figures 11 and 12 show the full-scale ship grounding simulation behaviors, with two rock positions, center of and 3.0m off the longitudinal center line, at free motion and plan constraint conditions in void, respectively. Contrary to the case of FSI analysis technique, it could be confirmed that grounding simulation behaviors and bottom damage in void conditions were very unrealistic.



(a) rock position center

(b) rock position 3.0 m off

Fig.11: Grounding response behaviors at free motion condition according to rock position in void

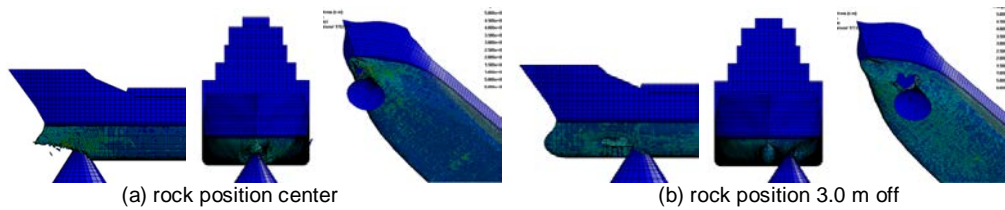


Fig. 12: Grounding simulation behaviors at plan constraint condition according to rock position in void

### 4.3 Investigation of collision accident between two ships

Striking cargo ship and struck deep-sea fishing vessel were collided on the way of typhoon evasion. The struck ship sank down after its side bottom structure was torn away by the bulbous bow's penetration of striking ship. Figure 13 shows the damage configurations and schematic damage drawings of the striking ship's forebody, and Fig. 14, of the struck ship's side superstructure and side bottom structure under free surface. From the investigation of all the collision damage informations, a collision scenario between the two ships was sketched, as shown in Fig. 15(a), where the forecastle bulwark of the striking ship hit and pushed the derrick post of the struck one at 2.75 m from the casing, and the fashion plate also pushed down the casing during the collision. Figure 15(b) depicts one collision scenario in a plan view among several ones, considering several attack angles, their speeds, and wind speeds and directions. Material properties of mild and high tensile steels for the striking and struck ships are summarized in Table 2.



Fig. 13: Collision damage configurations and schematic damage drawings of striking ship

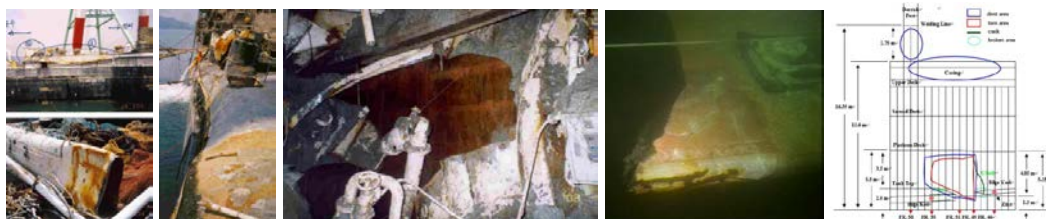


Fig. 14: Collision damage configuration and schematic damage drawings of struck ship

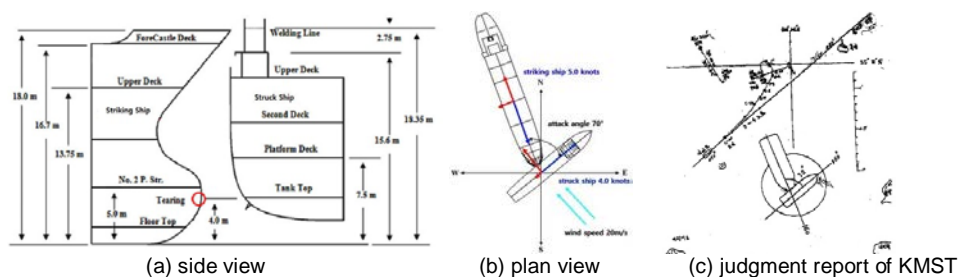


Fig. 15: Collision scenarios between two ships and judgment report of KMST

Figure 16 shows the full-scale ship collision simulation behaviors using FSI analysis technique, where the side bottom structure of the struck ship was penetrated by the bulbous bow of the striking one, and was torn away with around 4.0m x 4.0m in length and height, even though the forecastle of the striking ship extends over the bulbous bow by 1.55 m. This could be possible due to a little bit turnover of struck ship by the collision of forecastle to the derrick post and the pushdown of fashion plate to the casing in the seawater using FSI analysis technique. The bulbous bow was dented by the side frame structure and the bulkhead of the struck ship, and was torn away by the strong member, the tank top structure. This collision scenario and damage configuration could be confirmed by the judgment report of KMST, as shown in Fig. 15(c).



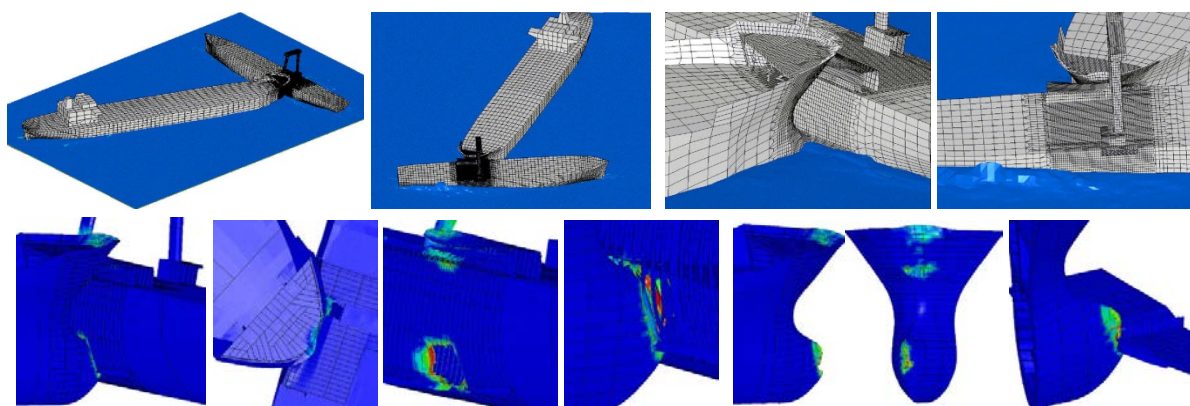
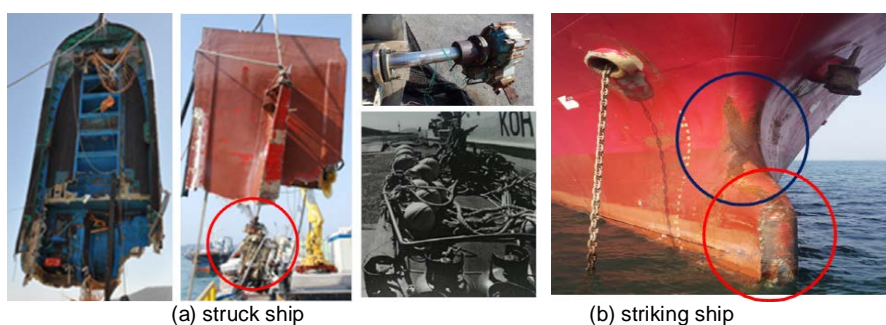


Fig. 16: Full-scale ship collision simulation behaviors & damage configurations using FSI analysis technique

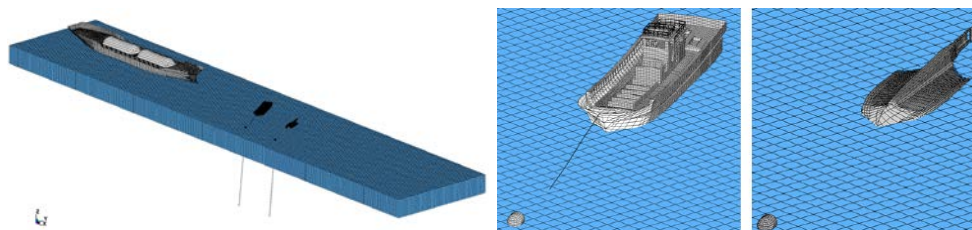
#### 4.4 Investigation of small fishing vessel collision accident

Small coastal grill net fishing vessel of G/T 9.77 ton was struck by a large LPG carrier with around G/T 3,000 ton during operation at night, broken in two bow and stern parts with wheelhouse upper plate, and sunk down to the bottom of river. Fishing vessel was moored with riding rope of mooring post on bow deck to fishing net cable of fixed gill nets. Figure 17(a) and (b) show the damage configurations of the struck and striking ships, respectively. The engine was rotated to the right, propeller shaft was bent from starboard side to port one, and starboard guardrail on the wheelhouse upper plate was also damaged. Paint on the bow flare of LPG carrier above the bulbous bow was scratched. The objective of this case was to investigate the cause of small fishing vessel collision accident whether it was struck by LPG carrier during floating upright or turned over states using FSI analysis technique, as shown in Fig. 17(c), by careful examination of their damages and of sea weather states at collision accident, such as current, wind and wave. Table 3 summarizes the material properties of mild steel, FRP, wood and foam for the striking and struck ships.



(a) struck ship

(b) striking ship



(c) striking and struck ship modeling using FSI analysis technique

Fig. 17: Damage configurations & full-scale ship collision simulation modeling using FSI analysis technique

Table 3: Material properties of mild steel, FRP, wood, foam

Property	Mild Steel	FRP	Wood	Foam
Young's modulus (GPa)	206.00	7.20	12.00	0.08
Density (kg/m <sup>3</sup> )	7,850.0	4,000.0	1,000.0	42.3
Yield & Ultimate stresses (MPa)	235.0 & 445.0	81.0 & 82.0	50.0 & 50.3	0.16 & 1.16
Failure strain	0.20, 0.25, 0.30	0.05~0.10	0.02~0.05	0.02~0.10
Dynamic yield stress constants	D=40.4 s <sup>-1</sup> , q=5	-	-	-

Figure 18 shows the full-scale ship collision simulation behaviors and damage configurations. It could be confirmed that the fishing vessel was struck by the LPG carrier under the floating upright state from

the several damage patterns and full-scale ship collision simulation behaviors using FSI analysis technique, such as more larger size of damage fracture of starboard side compared to the port side one, starboard guardrail damage of wheelhouse upper plate, right rotation of engine and bend direction of propeller shaft from starboard side to port one, and paint scratch in the upper bow of LPG carrier, etc. All these predictions could be possible from full-scale ship collision simulation using FSI analysis technique, not in void condition.

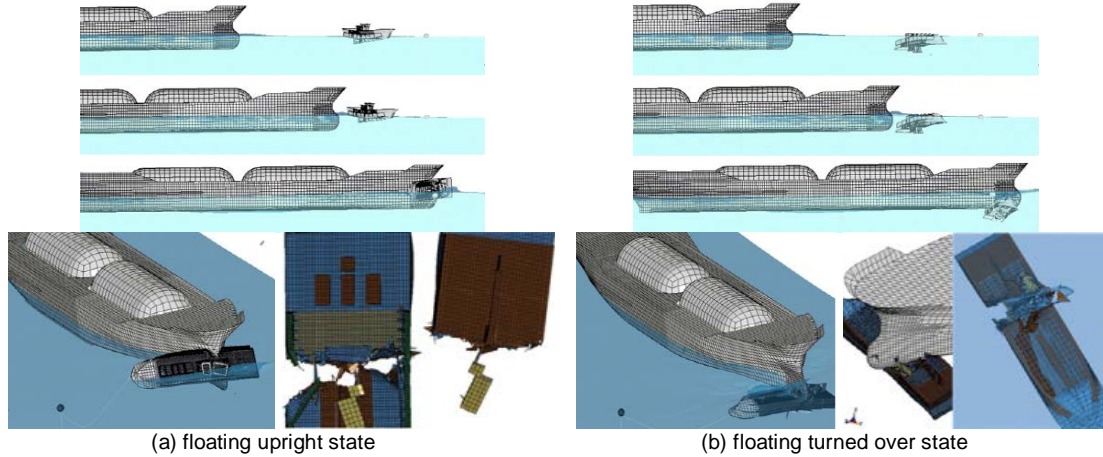


Fig. 18: Full-scale ship collision simulation behaviors & damage configurations using FSI analysis technique

#### 4.5 Investigation of flooding & sinking accident of ship under breaking wave

The ship with displacement 400 ton under the quay outfitting was flooded and sunk down due to the tidal breaking wave under the bomb cyclone, as shown in Fig. 19(a). Full-scale ship flooding & sinking simulation was carried using FSI analysis technique for the investigation of flooding procedure through the openings and the estimation of the flooding duration. From the marine meteorological information of the ocean data (mooring) buoy at a distance around 40.0km away from quay, significant wave height and period were 4.6 m and 8.0 sec, respectively. Figure 19(b) shows the ship and seawater model including quay, air and vertical dock fenders, ropes, etc., and the ship is floating in the seawater at the depth 7.3 m. There are many openings on the deck and superstructure, and in the watertight bulkheads, as shown in Fig. 19(c).

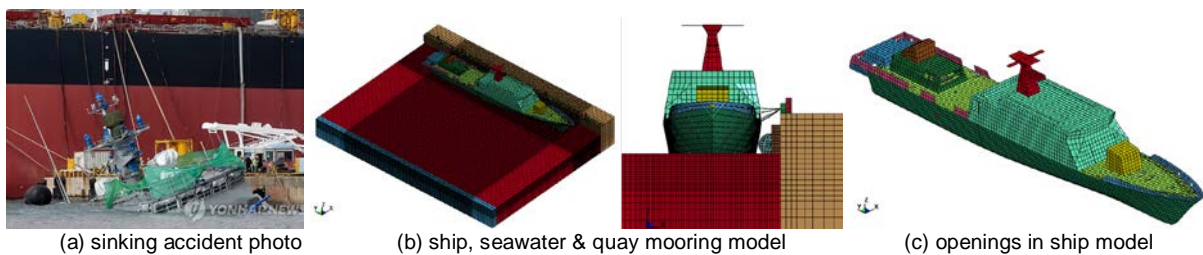


Fig. 19: Full-scale ship flooding & sinking simulation model and accident photo using FSI analysis technique

Due to very large computational time in this full-scale ship flooding & sinking simulation using FSI analysis technique, the simulation was carried out by three steps. At the first step, the ship showed more or less complicated motion of heaving, rolling and surging, and air fenders, also heaving and surging, as shown in Fig. 20(a). Even though the breaking wave escaped through the gaps in the bulwarks, a lot of seawater was still gathered on the deck surrounded by the bulwarks. It could be found that seawater flowed into the several openings of the deck and through the openings of the superstructure, and that the engine compartments became flooded gradually, as shown in Fig. 20(b).

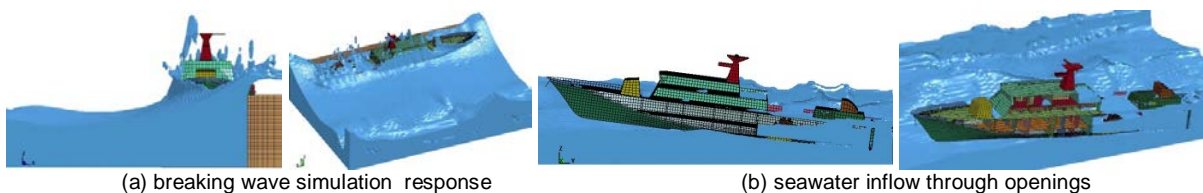


Fig.20: Breaking wave simulation behaviors & seawater inflow through openings of deck and superstructure



Figure 21 shows the breaking wave simulation behaviors to the ship and quay, and ship motion ones, depending on the breakage of the rear ropes at the second step. As the seawater flooded in the inboard of ship, the rear of the ship trimmed by the stern more and moved more vertically and laterally, and the 5th, 6th and 4th ropes were cut off one by one with the increase of their tensile strengths, where the rear of the ship rolled out more to the starboard. Seawater flowed inside through the doors of superstructure and the openings of deck, and propagated through the openings of watertight bulkheads to the accommodation compartments. Breaking wave also swept over the forecastle deck and seawater also flowed inside through the openings of forecastle deck into the inboard compartments.

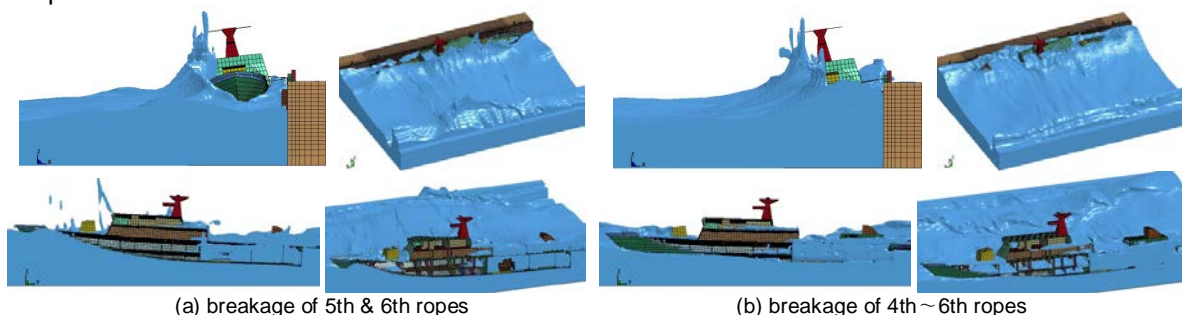


Fig.21: Breaking wave simulation behaviors with breakage of ropes, seawater inflow & propagation

At the final step, Fig. 22 shows the breaking wave simulation behaviors to the ship and quay, where the ship sank down more and rolled out more to the starboard. After seawater was flooded into the most compartments under the main deck, seawater flowed inside through the doors of superstructure, and the ship sank down more and the rear starboard bottom touched to the bottom. Through the full-scale ship flooding & sinking simulation using FSI analysis technique and realizing the rough sea condition, such as breaking wave, flooding and sinking accident procedure could be investigated with high accuracy.

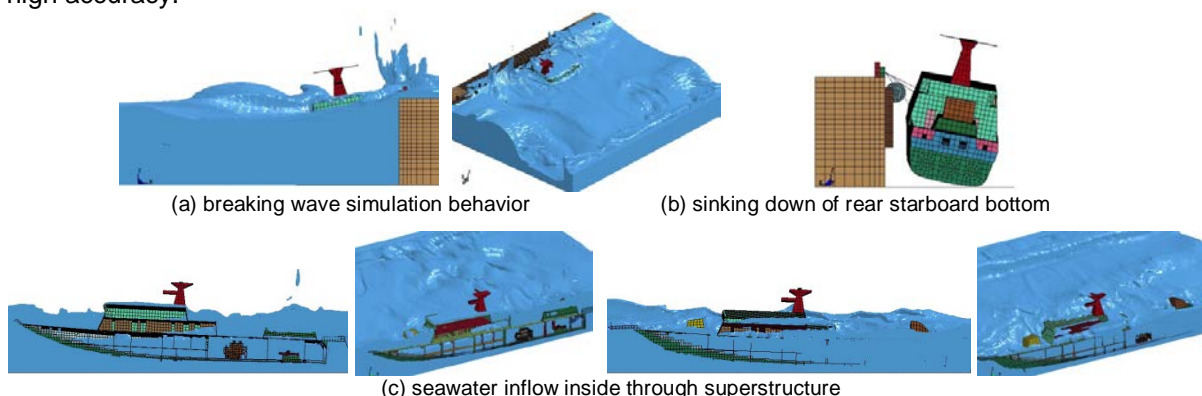


Fig.22: Breaking wave simulation behaviors, seawater inflow through doors & sinking down to bottom

#### 4.6 Investigation of deep-sea fishing vessel sinking accident

Deep-sea fishing vessel was fully flooded in the processing & working space, engine room and fish holds, and was sunk down due to the very rough sea weather during fishing operation in the Bering Sea, and many crews were dead and/or missed. Typical full-scale ship flooding & sinking simulation was carried out, and sinking process and cause was analyzed for the precise and scientific investigation of sinking accident using highly advanced M&S system of FSI analysis technique.

For the objective secure of weather and sea states in the Bering Sea, time-based wave and wind simulation at the region during sinking accident was carried out, as shown in Fig. 23(a). Sea and weather states were realized by simulating the irregular strong wave with significant wave height 4.5m & period 8.0sec, and irregular strong wind with wind speed 15.0m/sec, as shown in Fig. 23(b). Full-scale ship and fluid (air & seawater) modeling was performed for flooding & sinking simulation, investigating the hull form, structural arrangement & weight distribution through its drawings, figuring out the exterior inflow openings, interior flooding paths, as shown in Fig. 23(c), and the weight distributions of fish catch, fuel oils and their tanks through the stability calculation, and estimating the main tank capacity by its drawings and stability calculation and predicting their loading status by the daily report, as shown in Fig. 23(d).

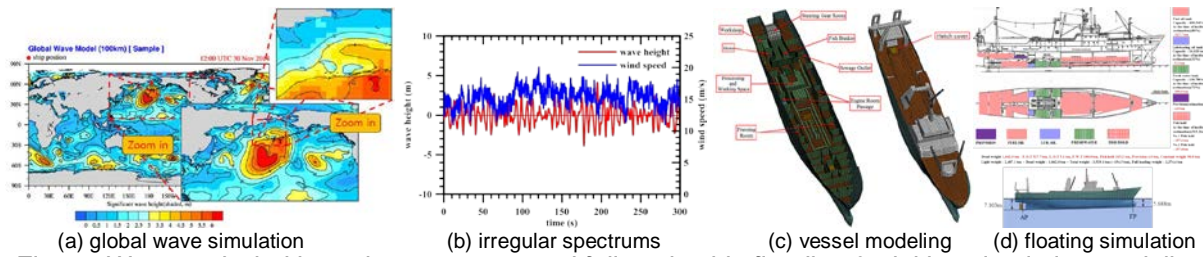


Fig.23: Wave and wind irregular spectrums and full-scale ship flooding & sinking simulation modeling

Full-scale ship flooding & sinking simulation was carried out for the seawater inflow through the exterior openings, hatch cover and sewage outlet, and through the interior paths along the compartments, processing & working space, engine room and fish holds together with the inclination to the starboard and port sides, the submergence of the stern under the surface, and the sinking to the bottom, greatly by two scenarios, as shown in Fig. 24.

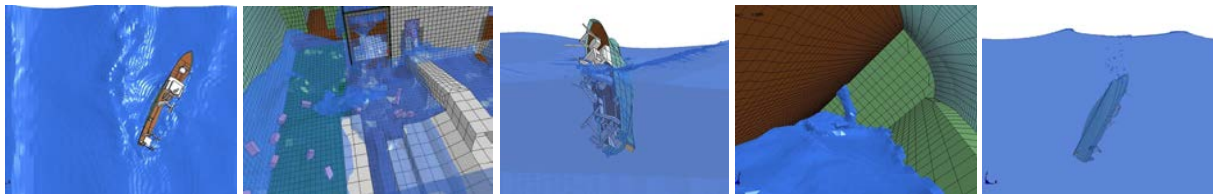


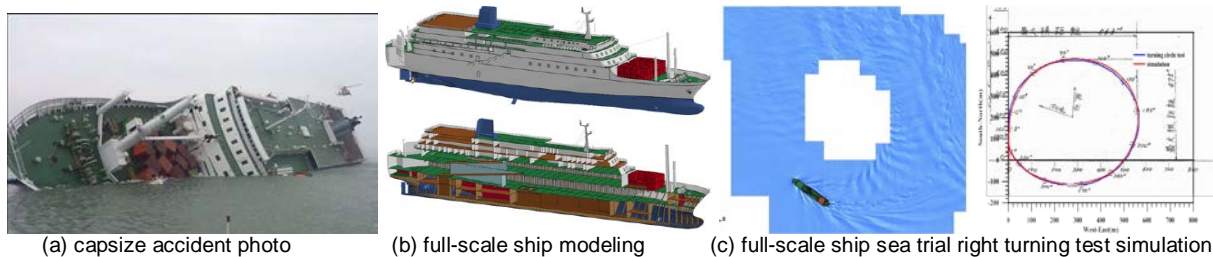
Fig.24: Full-scale deep-sea fishing vessel flooding & sinking simulation behaviors

It could be confirmed that the accident ship was flooding and sunk down from the full-scale ship flooding & sinking simulation behaviors using FSI analysis technique with a little bit different situation from the general capsized and sinking accident due to the simple loss of stability, in that the stern part subsided under the surface with the center of gravity descended a little bit down due to the seawater inflow in the engine room and fish holds, and with continued large angle of heel at the same time of submerged stern part under the surface even though its heel was progressed greatly.

#### 4.7 Investigation of ro-ro ferry ship capsized & sinking accident

Ro-Ro ferry ship was capsized and sunk down to the bottom in the seawater around Jindo-gun, as shown in Fig. 25(a), due to the rapid turning with several reasons, such as gravity rise due to excessive extension and rebuilding of stern part, lack of stability, shortage ballast and excessive cargo loading, excessive outward heel due to small GM during rapid turning, and cargo leaning according to lateral heel angle due to poor lashing, etc. Objective of this study is to investigate the initial stage of capsized accident cause at present using highly advanced M&S system of FSI analysis technology through the verification of full-scale ship turning simulation by comparison with maneuvering performance sea trial test result of initial building ship, as shown in Fig. 25(c).

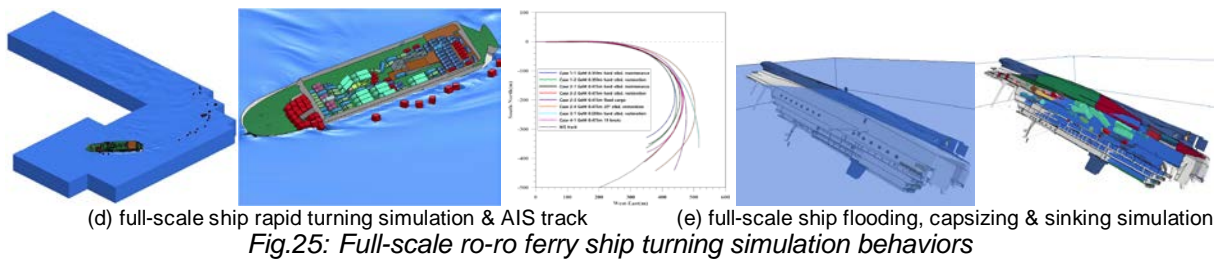
Full-scale ship rapid turning simulation was carried out, as shown in Fig. 25(d), considering several factors, such as GoM, ship velocity, rudder angle, etc., using full-scale ship and fluid (air & seawater) modeling, as shown in Fig. 25(b), accurate ship model modification using floating simulation according to hydrostatic characteristics of loading conditions, and investigation of cargo loading arrangement and cargo lashing states. There was relatively good agreement of full-scale ship sea trial turning simulation with sea trial test result, and good prediction of cargo loading arrangement and cargo lashing states was figured out comparing to the AIS track in this capsized accident. Figure 25(e) shows the full-scale ship flooding, capsizing and sinking simulation behaviors.



(a) capsized accident photo

(b) full-scale ship modeling

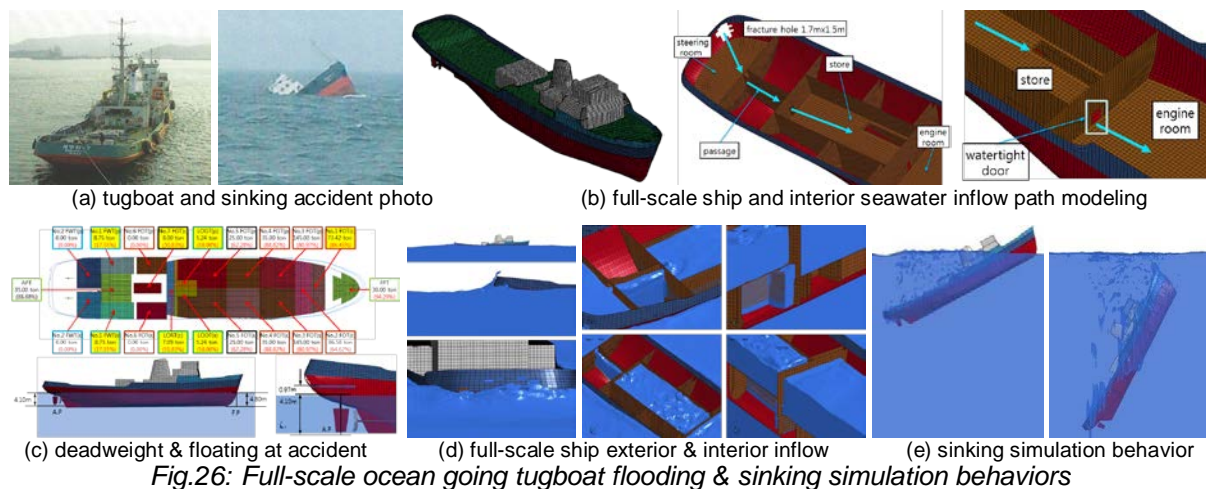
(c) full-scale ship sea trial right turning test simulation



#### 4.8 Investigation of ocean going tugboat sinking accident

Ocean going tugboat was fully flooded in the engine room with tearing puncture damage by the collision of 3 hold barges to the rear left steering room and steering gear failure, was sunk down without clear reasons in the sea during drift at the local time 8:15 in the morning, as shown in Fig. 26(a). Full-scale ship and interior seawater inflow path modeling, as shown in Fig. 26(b), and prediction of each tank and compartment volume were conducted by floating simulation using FSI analysis technique and hydrostatic characteristic program, as shown in Fig. 26(c), through estimation of hull form through its drawings, prediction of ship weight and buoyancy distribution of lightweight and full-loading departure conditions and the information of each tank through Trim & Stability Calculation, and careful analysis of fuel oil and fresh water transfer just before sinking accident. These several estimation and prediction processes are very important for the accurate cause investigation of the actual flooding & sinking accident.

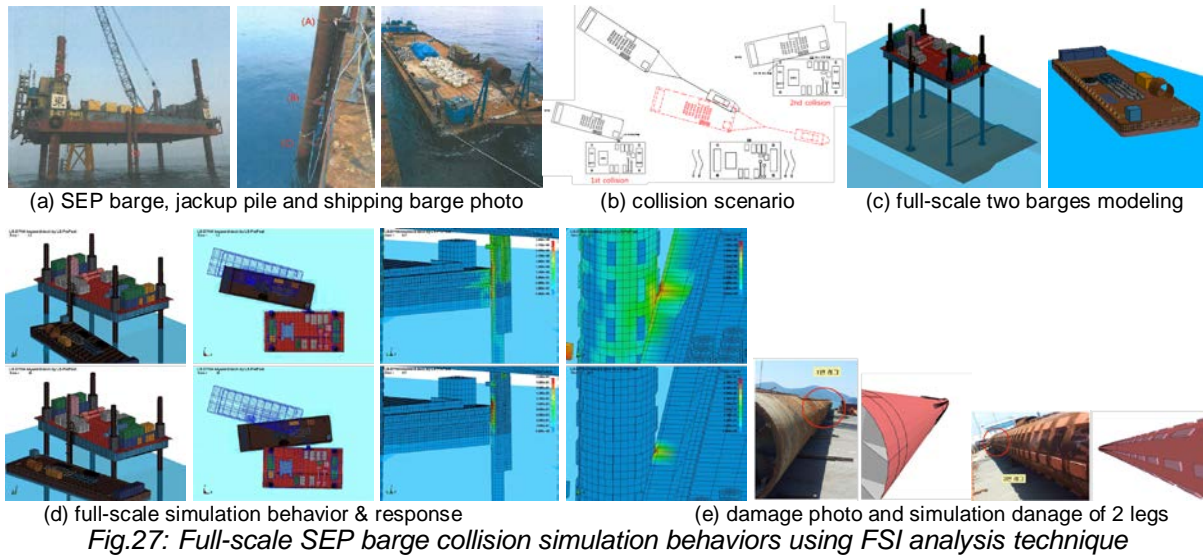
Full-scale ship flooding & sinking simulation was carried out, and sinking process and cause was analyzed for the precise and scientific investigation of sinking accident using highly advanced M&S system of FSI analysis technique. Figure 25(d) & (e) show the full-scale ship exterior & interior inflow procedures and sinking simulation behaviors in one of 3 cases, whose precise elapsed times could be predicted.



#### 4.9 Investigation of SEP barge collision accident

Jack-up pile of SEP(Self Elevated Pontoon) barge was collided very large at first, and then the 1st leg, slightly in the sea by the material shipping barge during coming alongside the barge, as shown in Fig. 27(a), where the 1st and 3rd legs were bent. Full-scale ship collision simulation was carried out using highly advanced M&S system of FSI analysis technique for the investigation of collision accident, figuring out the general shape, dimension and weight distributions of SEP barge and material shipping barge, and their detail structures through their drawings and photos, and submitted materials, estimating the sea bottom condition under the platform by comparing the total length of each leg and its topside one, and the leg housing structure mechanism for the restriction of top legs, predicting the collision simulation scenarios, as shown in Fig. 27(b), from the 1st and 2nd collision damages, and modeling full-scale ship and fluid (seawater and air), as shown in Fig. 27(c). Accurate cause investigation of collision accident was performed by the full-scale ship collision simulation, as shown in Fig. 27(d), and bent damage of legs was figured out, as shown in Fig. 27(e).





#### 4.10 Investigation of high speed passenger ship collision accident with whale

There happened several collision accidents of high speed passenger ship with underwater floating matters (whale), as shown in Fig. 28(a), where one passenger was died and a hundred ones, injured. Full-scale ship collision analysis of high speed passenger ship was performed with whales, as shown in Fig. 28(b) & (c), using FSI analysis technique for the cause investigation of collision accident, especially understanding of damage mechanisms due to the collision of its hydrofoil system with whale. Table 4 summarizes the material properties of aluminum alloy and stainless steel of high speed passenger ship and hydrofoil. Figure 28(d) shows the collision response behavior of passengers in the front and middle decks, and their acceleration responses according to deck position and dummy pattern. From this study, it could be confirmed that leverage of bulbous bow brought about more larger impact of foil & strut system to the ship structure and passenger, and led the bottom shell plate to be torn away and flooded. Seat belt was found to enhance the safety to the shock against the whale collision in the front deck.

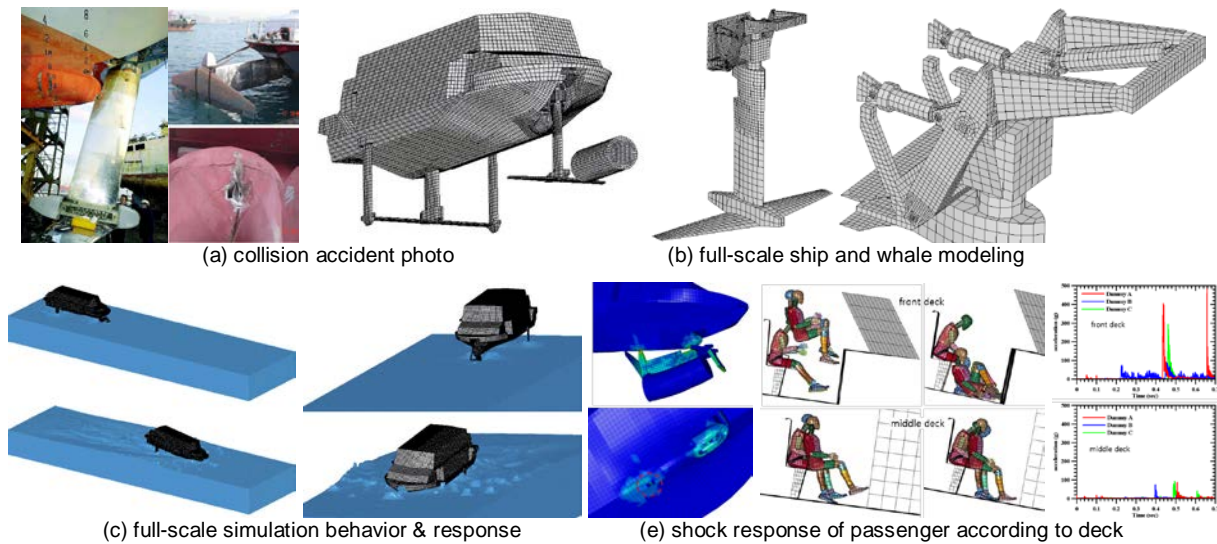


Table 4: Material properties of aluminum alloy and stainless steel

Property	Aluminum alloy	Stainless Steel
Young's modulus (GPa)	69.00	206.00
Density (kg/m <sup>3</sup> )	2,660.0	7,850.0
Yield & Ultimate stresses (MPa)	147.0 & 294.0	282.0 & 623.0
Failure strain	0.20~0.30	0.20~0.30
Dynamic yield stress constants	D=6,500 s <sup>-1</sup> , q=4	D=5,860 s <sup>-1</sup> , q=5

#### 4.11 Investigation of collision damage assessment of bulk carrier with container box

Damage was reported on the side structure shell of bulk carrier due to the collision accident by the unidentified floating or submerged matters (40 ft high cube container box), as shown in Fig. 29(a), where there were two blow point traces, ① and ②, and a inclined trace band between two points ① and ②, and 3 cracks at the 7 ~ 8 mm upper part ③ from inner bottom. Two blow points ① and ② were located around at 4.5 m under the free surface and 2.5 m upon the point ③. Localized indent was also predicted at blow point ②.

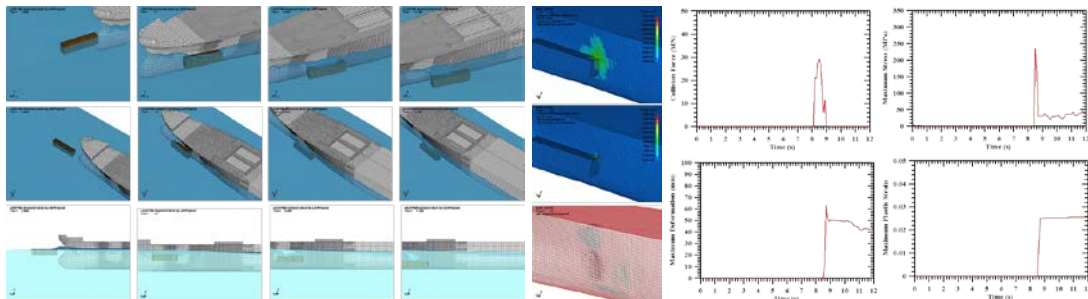
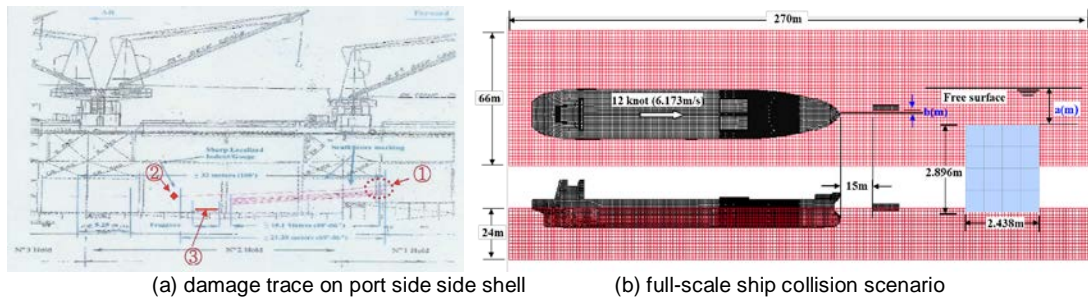
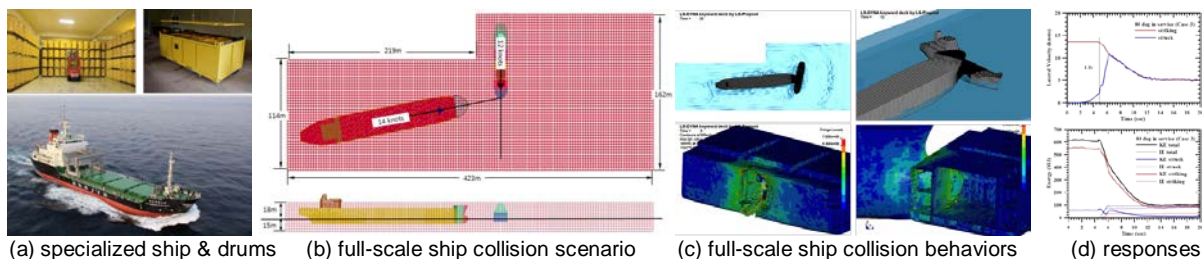


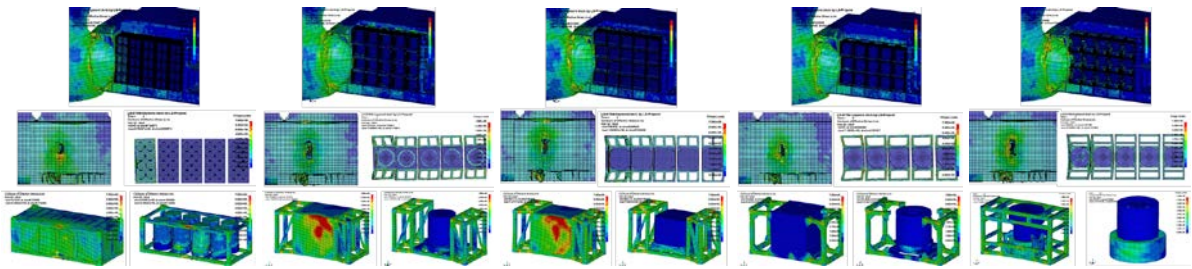
Fig.29: Full-scale bulk carrier collision simulation with container box using FSI analysis technique

From the full-scale ship collision simulation with container box according to collision scenario, as shown in Fig. 29(b), the following impact blow situations could be predicted. Floating container box on the free surface could be hardly collided to the bulk carrier bow side shell due to the wave making effect and squeezing pressure, and submerged container boxes, at 0.0 m ~ 0.1 m under the free surface and around 2.0 m off the longitudinal center line, as shown in Fig. 29(c), could be impacted only to the 1st blow point area and sunk down due to the very small buoyancy. There was no possibility for the 2nd impact and to the 2nd blow point, and also very small damage even at the 1st blow point area.

#### 4.12 structural safety assessment of specialized ship collision accident

Structural safety assessment was performed for the collision accidents of specialized ship structure and its cargo drums with DWT 2,600 ton, as shown in Fig. 30(a), using FSI analysis technique. Diverse scenarios were tried for the conservative safety assessment, such as several collision angles and 5 striking ship sizes from DWT 500 to 35,000 ton, and cargo container boxes and drums were also loaded inside the cargo hold of struck ship. Figure 30(b) & (c) typically show the collision scenario, simulation behaviors of DWT 35,000 ton striking ship, where striking ship collided to the front of its 3rd cargo hold in service at 80 degree attack angle, and Fig. 30(d), collision responses of lateral velocity, kinetic and internal energies of striking and struck ships.





(e) full-scale ship collision behaviors according to container box and drum

Fig.30: Full-scale specialized ship collision simulation with container box &amp; drum using FSI analysis technique

Full-scale ship collision simulation was carried out again for the structural safety assessment of cargo container boxes and drums, as shown in Fig. 30(e), where fracture damage in the side inner hull of struck ship was greatly reduced to a small rupture by the crashworthiness of container boxes and drums. It could be found that damage patterns were different according to the type of container box and drum. The specialized ship was also found to be superior to the crashworthiness of ship collision due to the wide double side hull space. There was no damage in cargo drums, and container boxes also greatly contributed to the crashworthiness of side structure.

## 5 Considerations

Through the full-scale ship collision, grounding, flooding, sinking and rapid turning simulations of marine accidents using Marine Accident Integrated Analysis System (highly advanced M&S system of FSI analysis technique), its usefulness could be reconfirmed for the scientific investigation of marine accidents and for the systematic reproduction of accidental damage procedure.

## 6 References

- [1] KMST, *KMST (Korea Maritime Safety Tribunal) Judgment Report (2002 ~ 2015)*, <https://data.kmst.go.kr/kmst/verdict/writtenVerdict/selectWrittenVerdict.do>.
- [2] LSTC, *LS-DYNA User's Manual, Version 971 R7*, Livermore Soft Technology Corp., USA, (2013).
- [3] Aquelet, N., Souli, M., and Olovsson, L., Euler–Lagrange coupling with damping effects: Application to slamming problems, *Computer Methods in Applied Mechanics and Engineering*, 195, (2006), 110–132.
- [4] Souli, M., Ouahsine, A., and Lewin, L., ALE formulation for fluid-structure interaction problems, *Computer Methods in Applied Mechanics and Engineering*, 190, (2000), 659-675.
- [5] Rodd, J., and Sikora, J., Double hull grounding experiments, *Proceedings of the 5th International Offshore and Polar Engineering Conference*, (1995), 446-456.
- [6] Lee, S.G., Lee, J.S. and Yoon, Y.H., Fracture criterion on shock response analysis, *Proceedings of the Annual Autumn Conference, SNAK*, (2014), 849-855.